Human Neonatal Naive CD4+ T Cells Have Enhanced Activation-Dependent Signaling Regulated by the microRNA miR-181a

Amy C. Palin[*], **Vasavi Ramachandran**[*], **Swati Acharya**[*], and **David B. Lewis**[*]

[*]Department of Pediatrics, Program in Immunology, and the Institute for Immunity, Transplantation and Infection, Stanford University School of Medicine, Stanford, CA 94305

Abstract

Human neonates have reduced and delayed CD4+ T-cell immunity to certain pathogens compared to older children and adults, but the mechanisms for these developmental differences in immune function remain poorly understood. We investigated the hypothesis that impaired human neonatal CD4+ T-cell immunity was due to reduced signaling by naive CD4+ T cells following engagement of the αβ-TCR/CD3 complex and CD28. Surprisingly, calcium flux following engagement of CD3 was significantly higher in neonatal naive CD4+ T cells from umbilical cord blood compared to naive CD4+ T cells from adult peripheral blood. Enhanced calcium flux was also observed in adult CD4+ recent thymic emigrants. Neonatal naive CD4+ T cells also had higher activation-induced Erk phosphorylation. The microRNA miR-181a, which enhances activation-induced calcium flux in murine thymocytes, was expressed at significantly higher levels in cord blood naive CD4+ T cells compared to adult cells. Overexpression of miR-181a in adult naive CD4+ T cells increased activation-induced calcium flux, implying that the increased miR-181a levels of cord blood naive CD4+ T cells contributed to their enhanced signaling. In contrast, AP-1-dependent transcription, which is downstream of Erk and required for full T-cell activation, was decreased in cord blood naive CD4+ T cells compared to adult cells. Thus, cord blood naive CD4+ T cells have enhanced activation-dependent calcium flux, indicative of the retention of a thymocyte-like phenotype. Enhanced calcium signaling and Erk phosphorylation are decoupled from downstream AP-1-dependent transcription, which is reduced and likely contributes to limitations of human fetal and neonatal CD4+ T-cell immunity.

Introduction

There is substantial evidence that human neonates have a limitation in CD4+ T-cell immunity, particularly for adaptive immune responses mediated by Th1 cells (1). Following primary HSV infection, the HSV-specific Th1 and CD4+ T-cell dependent antibody response are markedly diminished and delayed in appearance in neonates compared to adults (2, 3). Limitations in antigen-specific CD4+ T-cell function also likely contribute to the vulnerability of the neonate and infant to severe infection with *M. tuberculosis* (4), a pathogen for which Th1 immunity is essential in humans (5). Decreased effector function of naive CD4+ T cells of the neonate *in vivo* is also suggested by the lower incidence of acute graft-versus-host-disease (GVHD) after cord blood (CB) hematopoietic cell transplants compared to mobilized adult peripheral blood transplants (6, 7). As GVHD requires naive T-cell activation and a Th1 response (8), these clinical observations suggest a cell-autonomous limitation of CB T-cell immunity following allogeneic transplantation.

Address correspondence and reprint requests to Dr. David B. Lewis, Dept. of Pediatrics, Division of Immunology, Allergy, and Rheumatology, Stanford University School of Medicine, CCSR Building Room 3215a, 269 Campus Drive, Stanford, CA 94305-5164. dblewis@stanford.edu.

Consistent with reduced neonatal CD4$^+$ T-cell immunity *in vivo*, naive CD4$^+$ T cells from CB compared to those of adult peripheral blood (APB) have reduced expression of activation-induced proteins *in vitro*, including the cell surface molecules CD69 and CD154 (CD40 ligand) and the Th1 cytokine IFN-γ (9). In the case of CD154 and IFN-γ, reduced expression by naive CD4$^+$ T cells of CB is observed after both pharmacologic stimulation using the combination of calcium ionophore and PMA and more physiologic simulation with alloantigen, superantigen, or CD3 and CD28 mAbs ((9–13), and our unpublished observations). Reduced CD154 expression by neonatal CD4$^+$ T cells likely contributes to the impaired Th1 immune response (9), as CD154 is required for generation of antigen-specific Th1 cells (14).

IL-2 production by neonatal naive CD4$^+$ T cells is also significantly reduced compared to adult naive CD4$^+$ T cells after physiological activation with allogeneic dendritic cells (9). These findings are notable, given the observation that toxic shock syndrome toxin (TSST)-1-reactive T cells in infants infected with TSST-1 expressing *Staphylococcus aureus* strains have reduced proliferation and IL-2 production, both properties of anergic T cells (15, 16). These results suggest that neonatal naive CD4$^+$ T cells may have a tendency to become anergic following antigenic activation due, at least in part, to impaired IL-2 production. The mechanisms responsible for this phenotype remain unclear.

The full activation of naive CD4$^+$ T cells requires the engagement of the αβ-TCR/CD3 complex and CD28 by cognate peptide/MHC and CD80/CD86, respectively, a process that can mimicked by polyclonal treatment with anti-CD3 and anti-CD28 mAbs. This treatment results in activation of the tyrosine kinases Lck, ZAP-70, and phospholipase C (PLC)γ1. Activated PLCγ1, in turn, catalyzes production of the second messengers inositol triphosphate (IP$_3$) and diacylglycerol (DAG). Production of IP$_3$ stimulates calcium release from the endoplasmic reticulum, which initiates an influx of extracellular calcium through the calcium release activated calcium (CRAC) channel of the cell membrane. This increase in the free intracellular concentration of Ca^{2+} ([Ca^{2+}]$_i$) results in the calcineurin-dependent activation and nuclear translocation of the NFAT family of transcription factors (17).

DAG and other ZAP-70 derived signals activate Ras, which, in turn, activates Erk in a MAPK cascade that results in the generation of AP-1, a heterodimeric transcription factor of Fos and Jun proteins (18). The activation-dependent expression of cytokines, such as IL-2 and IFN-γ, and TNF ligand family members, such as CD154, by T cells requires *de novo* transcription of their cognate genes by the engagement of NFAT and AP-1 in promoter *cis*-elements (19–22). There is considerable evidence that the generation of calcium flux, and consequent NFAT activation in the absence of AP-1 activation, results in a program of gene transcription promoting anergy rather than a productive immune response (22–24).

Limitations at many steps in T-cell activation-induced signaling and cytokine gene transcription may contribute to decreased antigen-induced cytokine and CD154 expression by CD4$^+$ T cells of the fetus or neonate. In support of proximal signaling limitations, some studies of CB T cells have found reduced tyrosine phosphorylation of the tyrosine kinases, such as Lck and ZAP-70 (25) or PLCγ1 (26) following CD3 and CD28 mAb stimulation compared to T cells from APB. An important limitation of these studies and many others (reviewed in (1)) was that they did not directly compare naive (CD45RA^{high} CD45RO^{low}) CD4$^+$ T cells of CB with those from APB, but used unfractionated APB T cells instead, which have a substantial number of memory/effector cells. Because memory/effector T cells have distinct, often enhanced, activation-dependent signaling properties compared to naive T cells (27), this approach is not as informative for identifying true developmental limitations in signaling by naive T-cell populations. Limits imposed upon CD4$^+$ T-cell

immunity in neonates by developmental changes in activation-dependent signaling in naive $CD4^+$ T cells remain unclear.

Here, we tested the hypothesis that reduced signaling in naive $CD4^+$ T cells following engagement of the αβ-TCR/CD3 complex and CD28 contributes to limitations in $CD4^+$ T-cell immunity in the human neonate. Unexpectedly, we found that TCR-induced increases in $[Ca^{2+}]_i$ and Erk phosphorylation were higher in naive $CD4^+$ T cells from CB relative to those from APB. This enhanced calcium response was mediated, at least in part, by increased levels of the microRNA miR-181a in CB naive $CD4^+$ T cells, and reflects the retention by CB $CD4^+$ T cells of a thymocyte-like phenotype. This enhanced signaling was decoupled from downstream activation-dependent AP-1 induction. This reduced AP-1 activity in CB naive $CD4^+$ T cells may account for previous observations of decreased cytokine and CD154 production by these cells (9), as well as a tendency towards $CD4^+$ T-cell anergy rather than a productive immune response in neonates and young infants.

Materials and Methods

Blood mononuclear cell and naive CD4⁺ T-cell isolation

Blood was collected from healthy adult donors with informed consent in accordance with the requirements of the Stanford University Internal Review Board (IRB). Umbilical cord blood was collected from the placentas of healthy births that were term gestation, normal weight, and delivered vaginally at Lucile Packard Children's Hospital in accordance with IRB requirements. CB and APB were anticoagulated with preservative-free heparin sodium sulfate (Sigma, St. Louis, MO) and subjected to density gradient centrifugation using Ficoll-Hypaque (GE Healthcare Biosciences, Pittsburgh, PA) to isolate the mononuclear cell (MC) fraction. Unless otherwise indicated, naive $CD4^+$ T cells used in experiments were purified from MCs by magnetic-activated cell sorting after treatment with a Human Naive $CD4^+$ T Cell Negative Selection Kit II and application to paramagnetic LS columns (Miltenyi Biotec, Auburn, CA). Cells for miR-181a measurements were positively selected with a CD4 Selection Kit (Miltenyi), and FACS-sorted on a FACS Aria or modified FACS Vantage (both BD Biosciences, San Jose, CA). Naive $CD4^+$ T cells were sorted and defined as follows: $CD3^+$ (allophycocyanin (APC)-AlexaFluor 750-conjugated, clone OKT3, eBioscience, San Diego, CA, or APC-AlexaFluor750-conjugated clone S4.1, Invitrogen, Carlsbad, CA), $CD4^+$ (APC-conjugated, clone S3.5, Invitrogen), $CD45RA^+$ (FITC-conjugated, clone HI100, BD Biosciences), $CD45RO^-$ (PE-conjugated, clone UCHL1, Invitrogen) and 7-aminoactinomycin D^- (7AAD, BD Biosciences).

Fluorescent labeling and measurement of calcium flux

Purified naive $CD4^+$ T cells ($1x10^7$ cells/ml) were either incubated with 8.0 μg/ml of Alexa488 succinimidyl ester (Molecular Probes/Invitrogen) in PBS (Gibco/Invitrogen) or in PBS alone for 20 min at room temperature. Labeled cells were washed twice with HBSS with calcium and magnesium and without phenol red (Gibco/Invitrogen) with 1% heat-inactivated human AB serum (hAB) (Gemini Bioproducts, West Sacramento, CA) and combined with equivalent numbers of unlabeled naive $CD4^+$ T cells. The combined labeled and unlabeled cells were then stained with APC-conjugated CD19 (clone SJ25-C1, Invitrogen), CD8α (clone 3B5, Invitrogen), and CD45RO (clone UCHL1, BD Biosciences or Invitrogen) mAbs. After washing, cells ($1x10^7$/ml) in HBSS with 1.0 % hAB were incubated with indo-1 acetoxymethyl ester (Molecular Probes/Invitrogen) at a final concentration of 500 nM for 30 min at 37°C. After washing, cells were incubated in HBSS with 1.0 % hAB for another 30 min at room temperature and stained with 7AAD. Indo-1 emission at 346 and 330 nm was measured on a ultraviolet laser-equipped modified FACS Vantage or an LSR II instrument (both from BD Biosciences). Samples were equilibrated at

37°C for 10 min prior to data acquisition. A 30 s baseline was collected, followed by addition of 1:1000 (v/v) of OKT3 (CD3ε) mAb-containing ascites (Cocalico Biologicals, Reamstown, PA) at 30 s. After 2 min 45 s, 30 μg of goat anti-mouse Ig (Jackson Immunoresearch, West Grove, PA) or sheep anti-mouse Ig (Millipore, Danvers, MA) was added to cross-link surface bound CD3ε mAb. After 8 min, ionomycin (Sigma) was added at a final concentration of 1.0 μM, and after 10 min 15 s, acquisition was either terminated (for miRNA transfected samples) or EGTA was added at a final concentration of 5.0 mM and acquisition was terminated at 12 min 30 s. The peak and mean 330/346 nm ratios from the CD3 mAb cross-linking period was calculated using FlowJo software (Treestar, Ashland, OR).

Protein tyrosine kinase 7 surface staining of naive CD4^{+} T cells

Purified APB naive CD4^{+} T cells were stained with rat IgG monoclonal anti-human protein tyrosine kinase 7 (PTK7) (generated by Genovac, Freiburg, Germany) or, as a negative control, purified rat IgG (Sigma) for 20 min at room temperature. After blocking with 10% hAB serum, cells were incubated with PE-conjugated goat-anti-rat-IgG (Jackson Immunoresearch), followed by additional blocking by incubation with unlabeled rat IgG for 15 min at 4°C. For calcium flux assays, cells were stained with APC-conjugated CD19, CD8α, and CD45RO mAbs, as described above. 7AAD was added after washing, and samples were loaded with indo-1 acetoxymethyl ester and analyzed as described above. For miRNA expression analysis, PTK7^{+} and PTK7^{−} 7AAD^{−} CD3^{+} (APC-Alexa750, clone S41, Invitrogen or PE-Cy7 conjugated, clone UCHT1, eBioscience), CD4^{+} (PerCP-Cy5.5, clone SK3, BD Biosciences; Alexa700, clone OKT4, eBioscience; or APC-Alexa750-conjugated, clone S3.5, BD Biosciences) CD45RA^{+} (FITC-conjugated ,clone HI100, BD Biosciences), CD45RO^{−} (APC-conjugated, clone UCHL1, Invitrogen) cells were sorted using a BD FACS ARIA II.

Phospho-flow analysis

After isolation of CB or APB MCs by Ficoll-Hypaque gradient centrifugation as described above, cells were stained with CD3-Alexa700 (clone UCHT1, BD Biosciences), CD4-Alexa 488 (clone OKT4, eBioscience), and CD45RA-Qdot 605 (clone MEM-56, Invitrogen). Stained MCs (1×10^6/well) were incubated in RPMI (Mediatech, Manassas, VA) with 10% FBS (Atlanta Biologicals, Lawrenceville, GA) at 37°C in Maxisorb 96-well plates (Nunc, Thermo Scientific, Rockford, IL) previously coated overnight with 1.0 μg/ml of functional grade CD3 mAb (clone OKT3, eBioscience, San Diego, CA) and 2.5 μg/ml of CD28 mAb (clone CD28.2, eBioscience) in PBS for 10, 15, 30, and 60 min or with 250 nM ionomycin (Sigma) and 50 ng/ml of PMA (Sigma) for 1, 5, and 15 min. Cells were fixed with a final concentration of 1.5% paraformaldehyde (Electron Microscopy Sciences, Hatfield, PA) in PBS with 1.0 mM β-glycerol phosphate (Sigma) and 1.0 mM sodium orthovanadate (Sigma) for 10 min at room temperature. Cells were pelleted and resuspended in ice-cold methanol (Fisher, Waltham, MA), incubated at −20°C for 20 min or −80°C overnight, then washed twice in PBS with 0.5% BSA (HyClone Labs, Logan, UT). Samples were then blocked with 10% (v/v) hAB for 15 min at room temperature. Anti-phospho-Erk1/2 pT202/pT204 (PE-conjugated, clone 20a, BD Biosciences) was added and incubated for 30 min at room temperature. Cells were washed twice in PBS with 0.5% BSA, resuspended in 0.5% paraformaldehyde in PBS with 1% (w/v) BSA, and stored at 4°C in PBS with 0.5% paraformaldehyde and 0.5% BSA until analysis on a BD Biosciences LSR II instrument. Naive CD4^{+} T cells were defined as CD3^{+} CD4^{+} CD45RA^{+}.

AP-1-dependent transcription reporter gene activity

Naive CD4^{+} T cells were activated with 2.5 μg/ml of PHA (Sigma) for 19.5 h as previously described (28), and then transfected with plasmids (2.0 μg/1×10^6 cells) using a Neon

electroporation system (Invitrogen) set for 2400 V, 12 milliseconds, and 2 pulses. The AP-1 reporter plasmid (generous gift of O. Martinez, Stanford University) has 5 AP-1 binding sites from the metallothionein promoter subcloned into the human IL-2 minimal promoter in a pGL3 plasmid backbone. A β-actin luciferase plasmid (generous gift of G. Crabtree, Stanford University) was used as a control. pEGFP-N1 (Clontech, Mountain View, CA) was used to assess transfection efficiency by flow cytometry. Twenty-four hours after transfection, 2×10^5 cells were activated with CD3 and CD28 mAb-coated Dynabeads (Invitrogen) at a 1:1 bead to cell ratio, or with 250 nM ionomycin (Sigma) and 50 ng/ml PMA (Sigma) for 4 hours in a total volume of 100 μl. After 4 h, 100 μl of One-Glo reagent (Promega Biosystems, Madison, WI) was added to each well, and after 3 min of incubation lysates were read for 1.0 s on a luminometer (Veritas, Promega). Five transfection replicates were performed for each sample. Transfection efficiency and cell death were assessed by evaluation of the GFP signal measured on an Accuri C6 flow cytometer after staining with 7AAD and CD4-PE (clone S3.5, Invitrogen) and CD45RA-APC (clone MEM-56, Invitrogen) mAbs.

microRNA isolation and quantitative PCR analysis

RNA was isolated using a mirVana isolation kit (Ambion/Life Technologies, Carlsbad, CA) according to the manufacturer's protocol from purified naive CD4+ T cells. RNA was analyzed by quantitative PCR using a BioRad (Hercules, CA) CFX384 Real-Time System or an ABI 7900 system (ABI/Life Technologies) and TaqMan miRNA assays or gene-specific assays (Ambion). The fold-change and relative expression were calculated using the $\Delta\Delta C_t$ method. miRNAs were normalized to RNU48 and mRNAs to GAPDH.

Transfection of primary CD4+ T cells with pre-miRNAs

Purified naive CD4+ T cells (1×10^6 cells) in RPMI with 10% FBS were transfected with 75 μM of mirVana miR-181a mimic or a control, non-targeting miRNA mimic (all from Ambion), and 5% v/v siPort reagent (Ambion) in Opti-MEM medium (Gibco/Invitrogen) at room temperature, according to the manufacturer's protocol. Prior to transfection, the miRNAs were labeled with Cy3 using Label IT siRNA Tracker (Mirus Bio, Madison, WI) following the manufacturer's instructions. Total RNA was isolated for analysis after 24h and 48h of incubation, and calcium flux was measured after 48 h.

Activation of naive CD4+ T cells and total RNA isolation

MACS-purified naive CD4+ T cells were stimulated for 4 hours at 37°C at 2.0×10^7 cells/mL with 2.0 μg/mL anti-CD3 (clone OKT3, eBioscience) and 10.0 μg/mL anti-CD28 (clone CD28.2, eBioscience), cross-linked with 33 μg/mL goat anti-mouse IgG (Jackson Immunoresearch, West Grove, PA) in RPMI with 10% FBS. Unstimulated cells were incubated in RPMI with 10% FBS under the same conditions. After stimulation, cells were pelleted and lysed with Tri Reagent (Molecular Research Center, Cincinnati, OH). Samples were stored at −80°C prior to RNA isolation, which was performed according to the manufacturer's protocol.

Statistical analysis

Results were analyzed using GraphPad Prism software (GraphPad, San Diego, CA), with p-values < 0.05 considered significant. Unless otherwise specified, a two-tailed unpaired Student's t-test was used.

Results

Activation-induced calcium flux is higher in CB naive CD4^{+} T cells compared to APB naive CD4^{+} T cells

As activation-dependent calcium-dependent signaling is critical for inducing the *de novo* transcription of genes encoding cytokines and CD154 in CD4^{+} T cells (19, 29), we first determined if limitations in such signaling in CB CD4^{+} T cells might result in reduced expression of these gene products. We developed a flow cytometric assay in which naive CD4^{+} T-cell populations were either fluorescently labeled with Alexa488 succinimidyl ester (barcoded) or left unlabeled (Fig. S1) and then combined, permitting the two cell populations to be simultaneously stimulated and analyzed for calcium flux under the same conditions. The labeling procedure did not significantly affect the calcium flux compared to that of unlabeled cells from the same donor (Fig. S1). Using this approach, naive CD4^{+} T cells from CB versus APB were directly compared after the cross-linking of surface bound CD3 mAb. Unexpectedly, the peak (p=0.025) and mean (p=0.01) calcium flux following CD3 mAb cross-linking were higher in naive CB CD4^{+} T cells than in APB naive CD4^{+} T cells (n=3) (Fig. 1A, B, and data not shown). The labeling did not significantly affect calcium flux (p=0.98, Fig. 1C). In contrast, there was no difference in either the peak (p=0.31) or mean (p=0.21) calcium flux after the addition of the calcium ionophore, ionomycin (Fig. 1D and data not shown), indicating that the capacity for pharmacologically-induced calcium flux in these two CD4^{+} T-cell types was equivalent.

Activated-induced calcium flux is higher in RTEs than in mature naive CD4^{+} T cells of APB

The CB naive CD4^{+} T-cell compartment appears to be relatively enriched in RTEs, T cells that have recently completed their intrathymic maturation and have emigrated to the periphery, based on relatively high content of signal joint T-cell receptor excision circles (sjTRECs) (30) and high levels of surface expression of PTK7, a human CD4^{+} RTE marker (31). To determine whether RTEs of APB had similar signaling properties as CB naive CD4^{+} T cells, we compared calcium flux in PTK7^{+} and PTK7^{−} APB naive CD4^{+} T cells (Fig. 2A). Both the peak (Fig. 2B) and the mean (Fig. 2C) calcium flux after anti-CD3 mAb cross-linking were higher in PTK7^{+} cells than PTK7^{−} from the same donor (n=4) (p=0.029 and p=0.006, respectively). There was also no significant difference in peak calcium flux following addition of ionomycin (p=0.41, data not shown), indicating that RTEs and more mature naive CD4^{+} T cells had similar capacity to flux calcium after pharmacologic stimulation. Together, these results suggest that the enhanced calcium flux of CB naive CD4^{+} T cells and APB CD4^{+} RTEs reflect the retention of a thymocyte-like phenotype.

Erk phosphorylation is higher in naive CD4^{+} T cells from CB than APB

Phosphorylation of Erk1/2 is induced in response to TCR engagement and co-stimulation (32–34) and is critical for the AP-1-dependent transcription of genes involved in T-cell activation, so we next determined whether phosphorylation of Erk1/2 was also enhanced in CB naive CD4^{+} T cells compared to those of APB. pErk was detectable by 10 minutes after stimulation with plate-bound anti-CD3 and anti-CD28 mAbs, and the percent of cells positive for pErk (%pErk[+]) was significantly higher in CB after 15 and 30 minutes of stimulation (Fig. 3A), though %pErk[+] was similar after 60 minutes of stimulation. The change in mean fluorescent intensity (ΔMFI) was significantly higher (p<0.05) in CB after 15 minutes of stimulation (Fig. 3B). There was no significant difference in the percentage of pErk^{+} cells or ΔMFI in response to stimulation with ionomycin and PMA at 5 or 15 minutes after stimulation (Fig. 3C, D). Representative histograms for pErk in APB and CB are shown in Fig. 3E and F, respectively. These data indicate that the higher Erk phosphorylation observed in naive CD4^{+} T cells from CB compared to those of APB applied to physiologic, rather than pharmacologic activation.

Expression of miR-181a and its positive regulation of activation-induced calcium flux in CD4$^+$ T cells

The microRNA miR-181a has been reported to regulate calcium flux and Erk phosphorylation positively in murine CD4$^+$ T lineage cells, including in thymocytes, which highly express miR-181a (35). As CB naive CD4$^+$ T cells have features suggestive of an enrichment in RTEs and retention of a thymocyte-like signaling properties, we next investigated whether miR-181a contributes to increased $[Ca^{2+}]_i$. Expression of miR-181a was significantly higher in naive CD4$^+$ T cells of CB compared to those of APB (Fig. 4A, p=0.0076), as measured by quantitative PCR. Similarly, adult PTK7$^+$ RTEs had significantly higher miR-181a expression (p<0.05) than PTK7$^-$ naive CD4$^+$ T cells from the same donor (Fig. 4B), consistent with higher calcium flux in PTK7$^+$ than PTK7$^-$ cells. To determine if miR-181a positively regulates calcium flux in peripheral naive CD4$^+$ T cells, we chose to over-express miR-181a in naive CD4$^+$ T cells from APB, rather than inhibiting miR-181a in CB T cells, as others have reported difficulties in knocking down miR-181a (36). Overexpression was achieved by transient transfection with pre-miRNAs because preliminary studies using lentiviral vectors resulted in very low infection rates and required prolonged culture (data not shown). Transfection of APB naive CD4$^+$ T cells with pre-miR-181a resulted in a robust increase in mature miR-181a levels (Fig. 4C) and significantly increased the mean calcium flux (p=0.04) after CD3 mAb crosslinking compared to cells transfected with a non-targeting control (Fig. 4D, E). There was also a trend towards an increase in peak calcium flux for cells transfected with pre-miR-181a (Fig. 4F, p=0.11). We did not observe decreases in mRNAs of predicted miR-181a target phosphatases previously identified using murine T-lineage cells (35) (data not shown). Peak and mean calcium flux after addition of ionomycin were not different between pre-miR-181a and control-transfected cells (Fig. 4G and data not shown, p=0.63 and p=0.86, respectively), indicating that the enhancement of calcium flux by miR-181a was specific for that following αβ-TCR/CD3 activation. miR-181a over-expression did not affect the viability of the cells as measured by 7AAD staining of all cell events or lymphocytes (Fig. S2).

AP-1-dependent transcriptional activity is reduced in CB naive CD4$^+$ T cells

CB and neonatal naive CD4$^+$ T cells have previously been shown to have features of anergic cells, such as reduced IL-2 production and proliferation in certain contexts, such as following exposure to bacterial superantigen (15, 16). As anergy induction can result when intact calcium-dependent activation of NFAT occurs in the absence of CD28 engagement or transcriptional activity of AP-1 (23, 37–39), we evaluated AP-1 activity by performing transient transfection of an AP-1-dependent luciferase reporter gene. We found that CB naive CD4$^+$ T cells had significantly lower levels of AP-1-dependent transcription than APB naive CD4$^+$ T cells after CD3 and CD28 mAb stimulation (Fig. 5A, p=0.010). In contrast, there was no significant difference between these cell types for the low level of AP-1-dependent transcription that was detected in the absence of stimulation (Fig. 5A, p=0.12) or for the high levels of activity that were induced by ionomycin and PMA treatment (Fig. 5B, p=0.92). In addition, there was no significant difference between CB and APB CD4$^+$ T cells for a β-actin-promoter driven luciferase signal (Fig. 5C, p=0.89), indicating that differences in transfection efficiency did not account for these findings. Collectively, these results argued for the impairment of AP-1-dependent transcription in CB naive CD4$^+$ T cells specifically following αβ-TCR/CD3 and CD28 engagement rather than a limitation in the amount or functional competence of AP-1.

Upregulation of anergy genes in activated CB naïve CD4$^+$ T cells

Because reduced AP-1 induction is implicated in establishment of anergy, we examined the upregulation of genes characteristic of anergy in CB compared to APB naive CD4$^+$ T cells. GRAIL and Cbl-b are E3 ubiquitin ligases induced after activation of cells fated to become

anergic (38–40). We measured induction of these two mRNAs after 4 h of stimulation with CD3 and CD28 mAbs. Cbl-b was induced in CB naive CD4+ T cells following activation, while mRNA levels decreased in APB naive CD4+ T cells following activation (Fig. 5D). The difference was statistically significant (p=0.024). GRAIL mRNA was undetectable in all conditions assayed (data not shown). Thus, the induction of Cbl-b in CB naive CD4+ T cells provided more molecular evidence for the tendency of these cells to become anergic following activation.

Discussion

Human neonates have functionally decreased and delayed CD4+ T-cell immunity, including for Th1 responses, which likely contributes to their vulnerability to more severe infection by viruses and certain intracellular bacteria (1). The *de novo* CD4+ T-cell response to neoantigens requires full activation of naive CD4+ T cells after engagement of the αβ-TCR/CD3 complex and the CD28 co-stimulatory molecule and their proliferation and differentiation into effector and memory cells. In the current study, we investigated whether limitations in naive CD4+ T-cell activation could contribute to impaired neonatal CD4+ T-cell immunity. Unexpectedly, we found that CB naive CD4+ T cells had enhanced rather than decreased calcium responses in response to engagement of CD3, and this phenotype also applied to the RTE subset of adult naive CD4+ T cells. Similarly, phosphorylation of Erk was higher in CB naive CD4+ T cells. In contrast, CD3 and CD28 mAb-induced activation AP-1-mediated transcription, which is Erk dependent, was impaired in CB naive CD4+ T cells compared to those of APB. As expression of CD3, CD4, and CD28 is similar between APB and CB T cells (1), differences in surface receptor or co-receptor expression are unlikely to account for our results. Taken together, these results indicate that CB naive CD4+ T cells have a striking combination of both enhanced and decreased signal transduction events with activation, and that enhanced signaling is consistent with the retention of a thymocyte-like phenotype by CB naive CD4+ T cells and circulating adult CD4+ RTEs.

The enhanced calcium signaling by CB naive CD4+ T cells was accounted for by increased levels of miR-181a; overexpression of miR-181a in APB naive CD4+ T cells resulted in enhanced CD3 mAb-induced calcium flux. In murine T-lineage cells, miR-181a expression is highest in double-negative thymocytes followed by a progressive decline as these cells mature into CD4+ CD8+ thymocytes, CD4+ CD8− thymocytes, peripheral naive CD4+ T cells, and, finally, effector CD4+ T cells. Assuming that this pattern of miR-181a expression applies to human CD4+ T-lineage maturation, our finding of greater calcium flux by adult CD4+ RTEs compared to more mature naive CD4+ T cells of APB suggests a role for miR-181a in the enhanced calcium flux of RTEs, although this remains to be directly shown. Higher anti-CD3 mAb-induced calcium flux has been observed in circulating adult naive CD4+ T cells compared to memory CD4+ T cells (41), which may be explained by higher miR-181a expression in naive CD4+ T cells.

Although the kinetics of the thymic production of and peripheral turnover of CD4+ T cells in the neonate are not known, it is likely that CB peripheral CD4+ T cells are highly enriched in RTEs because of the high activity of the thymus during fetal gestation through 6 months of age (42). In previous studies, CB naive CD4+ T cells and CD4+ RTEs of APB have been shown to share a number of phenotypic features, including the expression of high levels of PTK7, sjTRECs, and CD31, and robust proliferative responses to IL-7 (31, 43). The finding of hyper-stimulable calcium flux by CB naive CD4+ T cells and adult RTEs, which for both cell types is likely mediated, at least in part, by miR-181a, is also consistent with the idea that this signal transduction pattern represents the retention of a functional thymocyte-like phenotype. These results also suggest that, as for PTK7 surface expression (31), a decrease

in TCR-induced calcium signaling may be part of the normal post-thymic maturation of the circulating neonatal naive and adult $CD4^+$ T-cell compartments (31, 44, 45). Consistent with our results, Gorozny and colleagues have found that miR-181a expression and Erk phosphorylation are reduced in naive $CD4^+$ T cells isolated from elderly people (46), who have a markedly reduced number of RTEs compared to younger adults.

In mice, miR-181a regulates calcium flux in $CD4^+$ T cells by downregulating a number of phosphatases that dephosphorylate Lck and Erk (35). In an MHC class II-restricted $\alpha\beta$-TCR transgenic murine system, miR-181a has been shown to enhance $\alpha\beta$-TCR/CD3-mediated calcium signaling and Erk phosphorylation resulting in increased positive and negative selection of $CD4^+$ $CD8^+$ (double-positive) thymocytes and increased activation of mature $CD4^+$ T cells for IL-2 production and proliferation (35). Our data support a similar mechanism in humans, as we have found increased Erk phosphorylation in CB naive $CD4^+$ T cells. In addition, the finding that miR-181a is highly expressed in adult $CD4^+$ $PTK7^+$ RTEs is consistent with the pattern of expression of miR-181a in murine T-lineage cells.

Robust initial responses by CB $CD4^+$ T cells, followed by apoptosis of effector cells have previously been reported (47). Our data are consistent with these findings, as CB naive $CD4^+$ T cells have high calcium flux, due, in part, to high expression of miR-181a. Pro-apoptotic effects of miR-181a have been reported in cancer cell lines (48–50), and over-expression of miR-181a sensitizes cell lines to a variety of apoptosis-inducing chemotherapy agents and increases their activation of Caspases 3 and 9 (49, 50). miR-181a has also been shown to target multiple anti-apoptotic Bcl2 family members (51). While some anti-apoptotic effects of miR-181a have been reported (52), the preponderance of published results suggests that high expression of this miRNA may mediate both the enhanced calcium flux and the high frequency of apoptosis of activated CB $CD4^+$ T cells. As shown in Fig. S2, we did not see effects of miR-181a over-expression on survival of APB naive $CD4^+$ T cells, but the effect of miR-181a on modulating post-activation apoptosis remains to be determined.

The observation that CB naive $CD4^+$ T cells have increased $\alpha\beta$-TCR/CD3-induced calcium flux but decreased AP-1-dependent transcription after CD3 and CD28 engagement is consistent with a signaling pattern that induces anergy rather than cell proliferation and production of IL-2 and other cytokines. Anergic murine $CD4^+$ T-cell clones or $\alpha\beta$-TCR transgenic primary $CD4^+$ T cells result from the presence of calcium-dependent activation of transcription by NFAT in the absence of Erk phosphorylation and transcription by AP-1; this signaling profile has been achieved using calcium ionophore treatment alone, or APCs displaying antigenic peptide/MHC complexes but lacking ligands for CD28 (23, 53–56). In support of this hypothesis, we found that Cbl-b, an E3 ubiquitin ligase necessary in early induction of anergy (39), was modestly upregulated in CB naive $CD4^+$ T cells after stimulation with anti-CD3 and anti-CD28, but was downregulated in APB naive $CD4^+$ T cells under the same conditions. The anergy-like signal transduction profile described here may account for the greater tendency of TSST-1-reactive $V\beta2^+$ CB naive $CD4^+$ T cells than APB cells to become anergic *in vitro* or *in vivo* following exposure to bacterial superantigen TSST-1 (15, 16). A tendency towards the induction of anergy rather than full effector function may also account for the observation that hematopoietic transplants with umbilical cord blood cells elicit fewer instances of Th1-mediated GVHD than do transplants with adult-derived cells (6, 7).

The observation that $\alpha\beta$-TCR/CD3 engagement simultaneously induces higher levels of calcium flux and Erk phosphorylation, but reduced AP-1 activity, indicates that there is a decoupling of Erk activation from AP-1 activity. Erk is an immediate upstream activator of Fos, a component of the AP-1 heterodimer (57), and Erk activity is negatively regulated by

death-associated protein kinase (DAPK), which sequesters phosphorylated Erk (pErk) in the cytoplasm and prevent its translocation to the nucleus where it directly activates Fos (58). As we have found that DAPK mRNA is more highly expressed in CB naive CD4^{+} T cells compared to those of APB (our unpublished data), it is plausible that DAPK may contribute to decreased AP-1-dependent transcription (57) as well as NF-κB-dependent transcription (59). Thus, these inhibitory effects of DAPK could explain the discrepancy between increased Erk activation and decreased AP-1 activity we have observed.

Following T-cell activation, AP-1 and NFAT proteins cooperate for the transcription of genes encoding CD154 (19, 60), IL-2 (22, 24), IL-4, IFN-γ (21), and many other cytokines. Impaired AP-1 induction in CB naive CD4^{+} T cells may, therefore, be an important contributor to impaired CD154, IL-2, and IFN-γ production following stimulation with superantigen or allogeneic dendritic cells (9, 15, 16). In addition to the signaling pattern, we have found that Cbl-b is induced in CB naive CD4^{+} T cells, providing more molecular evidence that these cells may become anergic upon stimulation. Importantly, our results do not exclude other factors in contributing to impaired IFN-γ gene expression, such increased DNA methylation of the IFN-γ gene (61), reduced levels of NFATc2 in unfractionated CB CD4^{+} T cells (62), and altered antigen-presenting cell function (63, 64).

As we have previously shown that adult CD4^{+} RTEs also display relatively impaired responses after αβ-TCR/CD3 engagement for IL-2 and IFN-γ production compared to more mature APB naive CD4^{+} T cells (31), it will be of interest to determine to what extent adult RTEs and CB naive CD4^{+} T cells share impairments in signal transduction involving the Erk/AP-1 pathway and a tendency for anergy rather than full activation. In the mouse, single-positive thymocytes do not produce IL-2 upon stimulation under conditions in which peripheral CD4^{+} T cells do (65), suggesting that a decoupling between TCR engagement and effector cytokine may be a characteristic of the late stage of thymocyte development. Thus, including human CD4^{+} single-positive mature thymocytes (CD4^{+} CD8^{−} CD3^{high} CD1a^{low}) (1515) in an analysis of signaling in peripheral naive CD4^{+} T cell populations may also help determine to what extent alterations in signaling reflect the retention by these peripheral CD4^{+} T-cell populations of a thymocyte phenotype.

In summary, we have observed a distinct activation-induced signal transduction profile in CB naive CD4^{+} T cells, with an increased calcium response, Erk phosphorylation, and expression of the Cbl-b anergy-promoting gene, but decreased AP-1-dependent transcription. The increase in calcium flux is mediated, at least in part, by increased expression of the microRNA miR-181a, which regulates calcium flux in murine CD4^{+} T cells, and, as we have shown here, in primary human CD4^{+} T cells and, based on studies by others, may also contribute to CB naive CD4^{+} T cells being prone to undergoing apoptosis. These features of increased activation-induced calcium flux and mR-181a levels are also found in APB naive CD4^{+} RTEs, which is consistent with likely high proportion of CB naive CD4^{+} T cells that are RTEs. Together, these results indicate that CB naive CD4^{+} T cells have a unique signaling pattern that may contribute to their impaired IFN-γ secretion capacity, as well as their tendency to become anergic in response to stimulation with superantigen. CB naive CD4^{+} T cells are not broadly hyporesponsive, despite impaired effector cell function. These findings also highlight, and provide evidence for, the need for peripheral maturation and regulation of TCR sensitivity during the late stages of intrathymic and early stages of post-thymic T-lineage cell development.

Supplementary Material

Refer to Web version on PubMed Central for supplementary material.

Acknowledgments

Abbreviations used in this article

|	
AAD	aminoactinomycin
APB	adult peripheral blood
APC	allophycocyanin
CB	cord blood
DAG	diacyl glycerol
GVHD	graft-versus-host disease
hAB	human AB serum
IP3	inositol triphosphate
MC	mononuclear cell
MFI	mean fluorescent intensity
miR	microRNA
PLC	phospholipase C
PTK7	protein tyrosine kinase 7
sjTRECs	signal joint T-cell receptor excision circles
TSST	toxic shock syndrome toxin

References

1. Lewis, DB.; Wilson, CB. Developmental Immunology and Role of Host Defenses in Fetal and Neonatal Susceptibility to Infection. In: Klein, JO.; Maldonado, Y.; Nizet, V.; Remington, JS.; Wilson, CB., editors. Infectious Diseases of the Fetus and Newborn. 7th ed. Philadelphia: Elsevier Saunders; 2011. p. 80-191.

2. Burchett SK, Corey L, Mohan KM, Westall J, Ashley R, Wilson CB. Diminished interferon-gamma production and lymphocyte proliferation in neonatal and postpartum primary herpes simplex virus infection. J. Infect. Dis. 1992; 165:813–818. [PubMed: 1314868]

3. Sullender WM, Miller JL, Yasukawa LL, Bradley JS, Black SB, Yeager AS, Arvin AM. Humoral and cell-mediated immunity in neonates with herpes simplex virus infection. J. Infect.Dis. 1987; 155:28–37. [PubMed: 3025306]

4. Smith S, Jacobs R, Wilson C. Immunobiology of childhood tuberculosis: A window on the ontogeny of cellular immunity. J Pediatr. 1997; 131:16–26. [PubMed: 9255187]

5. Alcais A, Fieschi C, Abel L, Casanova J-L. Tuberculosis in children and adults: two distinct genetic diseases. J. Exp. Med. 2005; 202:1617–1621. [PubMed: 16365144]

6. Rocha V, Wagner JE, Sobocinski KA, Klein JP, Zhang MJ, Horowitz MM, Gluckman E. Graft-versus-host disease in children who have received a cord-blood or bone marrow transplant from an

HLA-identical sibling. Eurocord and International Bone Marrow Transplant Registry Working Committee on Alternative Donor and Stem Cell Sources. N. Eng. J. Med. 2000; 342:1846–1854.

7. Ballen KK, Spitzer TR. The great debate: haploidentical or cord blood transplant. Bone Marrow Transplant. 2010; 46:323–329. [PubMed: 21042314]

8. Wolf D, von Lilienfeld-Toal M, Wolf AM, Schleuning M, von Bergwelt-Baildon M, Held SAE, Brossart P. Novel treatment concepts for graft-versus-host disease. Blood. 2012; 119:16–25. [PubMed: 21948301]

9. Chen L, Cohen AC, Lewis DB. Impaired allogeneic activation and T-helper 1 differentiation of human cord blood naive CD4 T cells. Biol. Blood Marrow Transplant. 2006; 12:160–171. [PubMed: 16443514]

10. Nonoyama S, Penix LA, Edwards CP, Lewis DB, Ito S, Aruffo A, Wilson CB, Ochs HD. Diminished expression of CD40 ligand by activated neonatal T cells. J. Clin. Invest. 1995; 95:66–75. [PubMed: 7814647]

11. Jullien P, Cron RQ, Dabbagh K, Cleary A, Chen L, Tran P, Stepick-Biek P, Lewis DB. Decreased CD154 expression by neonatal CD4+ T cells is due to limitations in both proximal and distal events of T cell activation. Int. Immunol. 2003; 15:1461–1472. [PubMed: 14645155]

12. Cantó E, Rodríguez-Sánchez JL, Vidal S. Naive CD4+ cells from cord blood can generate competent Th effector cells. Transplantation. 2005; 80:850–858. [PubMed: 16210975]

13. Gans HA, Yasukawa LL, Zhang CZ, Wakim RH, Rinki M, Dehovitz R, Arvin AM. Effects of interleukin-12 and interleukin-15 on measles-specific T-cell responses in vaccinated infants. Viral Immunol. 2008; 21:163–172. [PubMed: 18419254]

14. Jain A, Atkinson TP, Lipsky PE, Slater JE, Nelson DL, Strober W. Defects of T-cell effector function and post-thymic maturation in X-linked hyper-IgM syndrome. J. Clin. Invest. 1999; 103:1151–1158. [PubMed: 10207167]

15. Takahashi N, Imanishi K, Nishida H, Uchiyama T. Evidence for immunologic immaturity of cord blood T cells. Cord blood T cells are susceptible to tolerance induction to in vitro stimulation with a superantigen. J. Immunol. 1995; 155:5213–5219. [PubMed: 7594532]

16. Takahashi N, Kato H, Imanishi K, Miwa K, Yamanami S, Nishida H, Uchiyama T. Immunopathophysiological aspects of an emerging neonatal infectious disease induced by a bacterial superantigen. J. Clin. Invest. 2000; 106:1409–1415. [PubMed: 11104794]

17. Lewis RS. Calcium signaling mechanisms in T lymphocytes. Ann. Rev. Immunol. 2001; 19:497–521. [PubMed: 11244045]

18. Smith-Garvin JE, Koretzky GA, Jordan MS. T cell activation. Ann. Rev. Immunol. 2009; 27:591–619. [PubMed: 19132916]

19. Schubert LA, King G, Cron RQ, Lewis DB, Aruffo A, Hollenbaugh D. The human gp39 promoter. Two distinct nuclear factors of activated T cell protein-binding elements contribute independently to transcriptional activation. J. Biol. Chem. 1995; 270:29624–29627. [PubMed: 8530342]

20. Tsytsykova AV, Tsitsikov EN, Geha RS. The CD40L promoter contains nuclear factor of activated T cells-binding motifs which require AP-1 binding for activation of transcription. J. Biol.Chem. 1996; 271:3763–3770. [PubMed: 8631992]

21. Penix LA, Sweetser MT, Weaver WM, Hoeffler JP, Kerppola TK, Wilson CB. The proximal regulatory element of the interferon-gamma promoter mediates selective expression in T cells. J. Biol. Chem. 1996; 271:31964–31972. [PubMed: 8943243]

22. Macián F, López-Rodríguez C, Rao A. Partners in transcription: NFAT and AP-1. Oncogene. 2001; 20:2476–2489. [PubMed: 11402342]

23. Macián F, García-Cózar F, Im S-H, Horton HF, Byrne MC, Rao A. Transcriptional mechanisms underlying lymphocyte tolerance. Cell. 2002; 109:719–731. [PubMed: 12086671]

24. Macián F, García-Rodríguez C, Rao A. Gene expression elicited by NFAT in the presence or absence of cooperative recruitment of Fos and Jun. EMBO J. 2000; 19:4783–4795. [PubMed: 10970869]

25. Sato K, Nagayama H, Takahashi TA. Aberrant CD3- and CD28-mediated signaling events in cord blood T cells are associated with dysfunctional regulation of Fas ligand-mediated cytotoxicity. J. Immunol. 1999; 162:4464–4471. [PubMed: 10201983]

26. Miscia S, Di Baldassarre A, Sabatino G, Bonvini E, Rana RA, Vitale M, Di Valerio V, Manzoli FA. Inefficient phospholipase C activation and reduced Lck expression characterize the signaling defect of umbilical cord T lymphocytes. J. Immunol. 1999; 163:2416–2424. [PubMed: 10452976]

27. Chandok MR, Farber DL. Signaling control of memory T cell generation and function. Sem. Immunol. 2004; 16:285–293.

28. Cron RQ, Schubert LA, Lewis DB, Hughes CC. Consistent transient transfection of DNA into non-transformed human and murine T-lymphocytes. J. Immunol. Meth. 1997; 205:145–150.

29. Oh-hora M, Rao A. Calcium signaling in lymphocytes. Curr. Opin. Immunol. 2008; 20:250–258. [PubMed: 18515054]

30. Marcolino I, Przybylski GK, Koschella M, Schmidt CA, Voehringer D, Schlesier M, Pircher H. Frequent expression of the natural killer cell receptor KLRG1 in human cord blood T cells: correlation with replicative history. Eur. J. Immunol. 2004; 34:2672–2680. [PubMed: 15368283]

31. Haines CJ, Giffon TD, Lu L-S, Lu X, Tessier-Lavigne M, Ross DT, Lewis DB. Human CD4+ T cell recent thymic emigrants are identified by protein tyrosine kinase 7 and have reduced immune function. J. Exp. Med. 2009; 206:275–285. [PubMed: 19171767]

32. Atherfold PA, Norris MS, Robinson PJ, Gelfand EW, Franklin RA. Calcium-induced ERK activation in human T lymphocytes. Mol. Immunol. 1999; 36:543–549. [PubMed: 10475609]

33. Franklin RA, Atherfold PA, McCubrey JA. Calcium-induced ERK activation in human T lymphocytes occurs via p56(Lck) and CaM-kinase. Mol. Immunol. 2000; 37:675–683. [PubMed: 11164895]

34. Nunès JA, Collette Y, Truneh A, Olive D, Cantrell DA. The role of p21ras in CD28 signal transduction: triggering of CD28 with antibodies, but not the ligand B7-1, activates p21ras. J. Exp. Med. 1994; 180:1067–1076. [PubMed: 7520466]

35. Li Q-J, Chau J, Ebert PJR, Sylvester G, Min H, Liu G, Braich R, Manoharan M, Soutschek J, Skare P, Klein LO, Davis MM, Chen C-Z. miR-181a is an intrinsic modulator of T cell sensitivity and selection. Cell. 2007; 129:147–161. [PubMed: 17382377]

36. Cuesta R, Martinez-Sanchez A, Gebauer F. miR-181a Regulates Cap-Dependent Translation of p27kip1 mRNA in Myeloid Cells. Mol. Cell. Biol. 2009; 29:2841–2851. [PubMed: 19273599]

37. Bandyopadhyay S, Duré M, Paroder M, Soto-Nieves N, Puga I, Macián F. Interleukin 2 gene transcription is regulated by Ikaros-induced changes in histone acetylation in anergic T cells. Blood. 2007; 109:2878–2886. [PubMed: 17148585]

38. Anandasabapathy N, Ford GS, Bloom D, Holness C, Paragas V, Seroogy C, Skrenta H, Hollenhorst M, Fathman CG, Soares L. GRAIL: an E3 ubiquitin ligase that inhibits cytokine gene transcription is expressed in anergic CD4+ T cells. Immunity. 2003; 18:535–547. [PubMed: 12705856]

39. Jeon M-S, Atfield A, Venuprasad K, Krawczyk C, Sarao R, Elly C, Yang C, Arya S, Bachmaier K, Su L, Bouchard D, Jones R, Gronski M, Ohashi P, Wada T, Bloom D, Fathman CG, Liu Y-C, Penninger JM. Essential role of the E3 ubiquitin ligase Cbl-b in T cell anergy induction. Immunity. 2004; 21:167–177. [PubMed: 15308098]

40. Bandyopadhyay S, Soto-Nieves N, Macián F. Transcriptional regulation of T cell tolerance. Semin. Immunol. 2007; 19:180–187. [PubMed: 17387022]

41. Roederer M, Bigos M, Nozaki T, Stovel RT, Parks DR, Herzenberg LA. Heterogeneous calcium flux in peripheral T cell subsets revealed by five-color flow cytometry using log-ratio circuitry. Cytometry. 1995; 21:187–196. [PubMed: 8582239]

42. Weerkamp F, de Haas EF, Naber BA, Comans-Bitter WM, Bogers AJ, van Dongen JJ, Staal FJ. Age-related changes in the cellular composition of the thymus in children. J. Allergy Clin. Immunol. 2005; 115:834–840. [PubMed: 15806007]

43. Kohler S, Thiel A. Life after the thymus: CD31+ and CD31- human naive CD4+ T-cell subsets. Blood. 2009; 113:769–774. [PubMed: 18583570]

44. Hassan J, Reen DJ. IL-7 promotes the survival and maturation but not differentiation of human post-thymic CD4+ T cells. Eur. J. Immunol. 1998; 28:3057–3065. [PubMed: 9808174]

45. Webb LM, Foxwell BM, Feldmann M. Interleukin-7 activates human naive CD4+ cells and primes for interleukin-4 production. Eur. J. Immunol. 1997; 27:633–640. [PubMed: 9079802]

46. Li G, Yu M, Lee W-W, Tsang M, Krishnan E, Weyand CM, Goronzy JJ. Decline in miR-181a expression with age impairs T cell receptor sensitivity by increasing DUSP6 activity. Nat. Med. 2012; 18:1518–1524. [PubMed: 23023500]

47. Thornton CA, Upham JW, Wikström ME, Holt BJ, White GP, Sharp MJ, Sly PD, Holt PG. Functional maturation of CD4+CD25+CTLA4+CD45RA+T regulatory cells in human neonatal T cell responses to environmental antigens/allergens. J. Immunol. 2004; 173:3084–3092. [PubMed: 15322168]

48. Fei J, Li Y, Zhu X, Luo X. miR-181a Post-Transcriptionally Downregulates Oncogenic RalA and Contributes to Growth Inhibition and Apoptosis in Chronic Myelogenous Leukemia (CML). PLoS One. 2012; 7:e32834. [PubMed: 22442671]

49. Galluzzi L, Morselli E, Vitale I, Kepp O, Senovilla L, Criollo A, Servant N, Paccard C, Hupé P, Robert T, Ripoche H, Lazar V, Harel-Bellan A, Dessen P, Barillot E, Kroemer G. miR-181a and miR-630 Regulate Cisplatin-Induced Cancer Cell Death. Cancer Res. 2010; 70:1793–1803. [PubMed: 20145152]

50. Bai H, Cao Z, Deng C, Zhou L, Wang C. miR-181a sensitizes resistant leukaemia HL-60/Ara-C cells to Ara-C by inducing apoptosis. J. Cancer Res. Clin. Oncol. 2012; 138:595–602. [PubMed: 22209977]

51. Ouyang Y-B, Lu Y, Yue S, Giffard RG. miR-181 targets multiple Bcl-2 family members and influences apoptosis and mitochondrial function in astrocytes. Mitochondrion. 2012; 12:213–219. [PubMed: 21958558]

52. Lwin T, Lin J, Choi YS, Zhang X, Moscinski LC, Wright KL, Sotomayor EM, Dalton WS, Tao J. Follicular dendritic cell-dependent drug resistance of non-Hodgkin lymphoma involves cell adhesion-mediated Bim down-regulation through induction of microRNA-181a. Blood. 2010; 116:5228–5236. [PubMed: 20841506]

53. Gajewski TF, Qian D, Fields P, Fitch FW. Anergic T-lymphocyte clones have altered inositol phosphate, calcium, and tyrosine kinase signaling pathways. Proc. Natl. Acad. Sci. U.S.A. 1994; 91:38–42. [PubMed: 7506419]

54. Morton AM, McManus B, Garside P, Mowat AM, Harnett MM. Inverse Rap1 and phospho-ERK expression discriminate the maintenance phase of tolerance and priming of antigen-specific CD4+ T cells in vitro and in vivo. J. Immunol. 2007; 179:8026–8034. [PubMed: 18056342]

55. Doherty M, Osborne DG, Browning DL, Parker DC, Wetzel SA. Anergic CD4+ T cells form mature immunological synapses with enhanced accumulation of c-Cbl and Cbl-b. J. Immunol. 2010; 184:3598–3608. [PubMed: 20207996]

56. Chiodetti L, Choi S, Barber DL, Schwartz RH. Adaptive tolerance and clonal anergy are distinct biochemical states. J. Immunol. 2006; 176:2279–2291. [PubMed: 16455984]

57. Kamal M, Pawlak A, BenMohamed F, Valanciuté A, Dahan K, Candelier M, Lang P, Guellaën G, Sahali D. C-mip interacts with the p85 subunit of PI3 kinase and exerts a dual effect on ERK signaling via the recruitment of Dip1 and DAP kinase. FEBS Let. 2010; 584:500–506. [PubMed: 20018188]

58. Chen C-H, Wang W-J, Kuo J-C, Tsai H-C, Lin J-R, Chang Z-F, Chen R-H. Bidirectional signals transduced by DAPK-ERK interaction promote the apoptotic effect of DAPK. EMBO J. 2005; 24:294–304. [PubMed: 15616583]

59. Chuang Y-T, Fang L-W, Lin-Feng M-H, Chen R-H, Lai M-Z. The tumor suppressor death-associated protein kinase targets to TCR-stimulated NF-kappa B activation. J. Immunol. 2008; 180:3238–3249. [PubMed: 18292548]

60. Noel G, Brinster C, Semana G, Bruniquel D. Modulation of the TCR stimulation strength can render human activated CD4+ T cells suppressive. Int. Immunol. 2009; 21:1025–1036. [PubMed: 19625380]

61. White GP, Watt PM, Holt BJ, Holt PG. Differential patterns of methylation of the IFN-gamma promoter at CpG and non-CpG sites underlie differences in IFN-gamma gene expression between human neonatal and adult CD45RO- T cells. J. Immunol. 2002; 168:2820–2827. [PubMed: 11884451]

62. Kadereit S, Junge GR, Kleen T, Kozik MM, Kaminski BA, Daum-Woods K, Fu P, Tary-Lehmann M, Laughlin MJ. Deficient IFN-gamma expression in umbilical cord blood (UCB) T cells can be

rescued by IFN-gamma-mediated increase in NFATc2 expression. J. Clin. Immunol. 2003; 23:485–497. [PubMed: 15031636]

63. Naderi N, Pourfathollah AA, Alimoghaddam K, Moazzeni SM. Cord blood dendritic cells prevent the differentiation of naïve T-helper cells towards Th1 irrespective of their subtype. Clin. Exp. Med. 2009; 9:29–36. [PubMed: 18979063]

64. Trivedi HN, HayGlass KT, Gangur V, Allardice JG, Embree JE, Plummer FA. Analysis of neonatal T cell and antigen presenting cell functions. Hum. Immunol. 1997; 57:69–79. [PubMed: 9438198]

65. Chang JF, Thomas CA, Kung JT. Induction of high level IL-2 production in CD4+8-T helper lymphocytes requires post-thymic development. J Immunol. 1991; 147:851–859. [PubMed: 1677670]
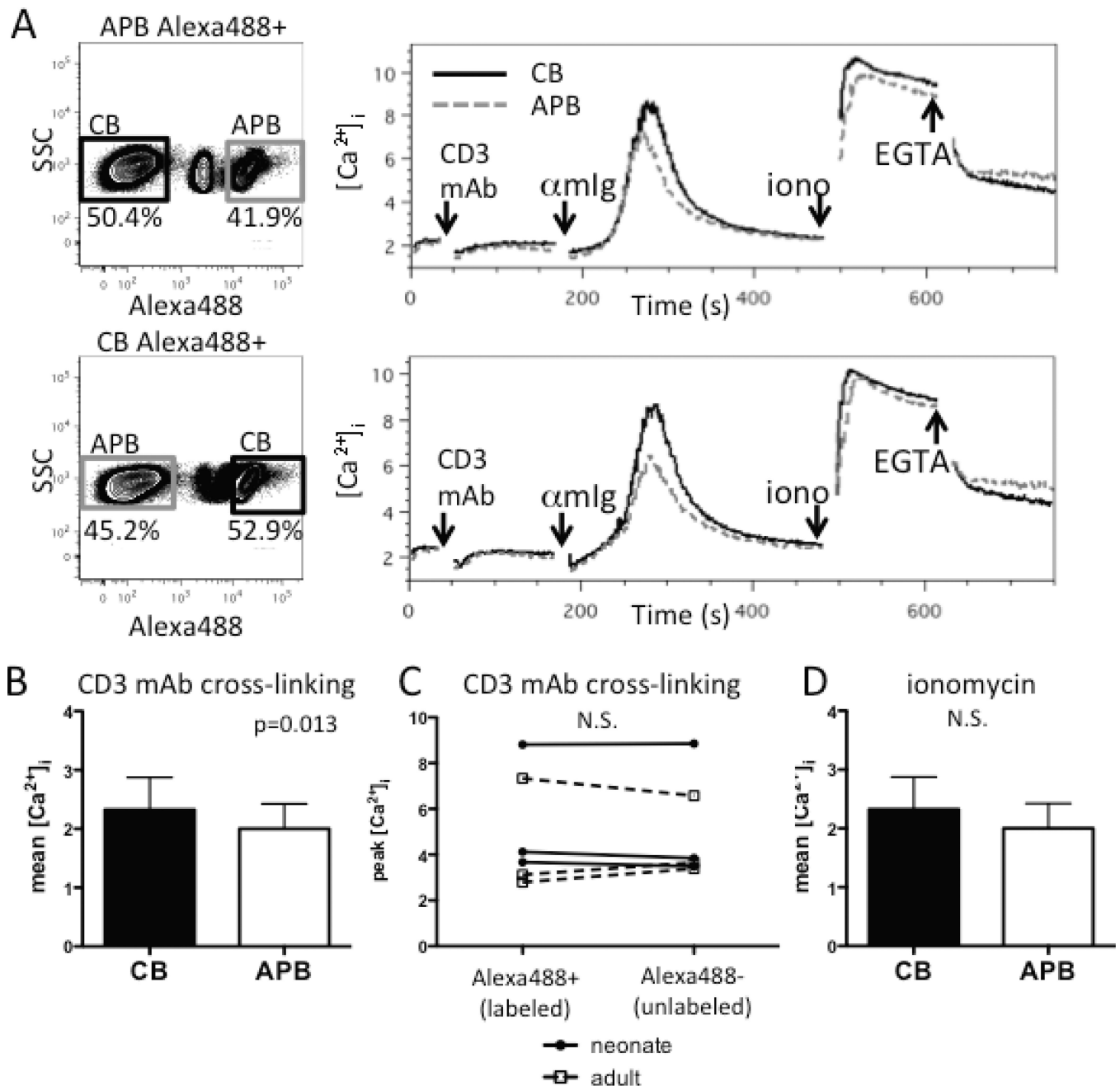
FIGURE 1.
Naive CD4^{+} T cells of CB have a higher calcium flux than APB naive CD4^{+} T cells after CD3 mAb cross-linking using anti-mouse IgG (αmIg). (**A**) Representative flow cytometry plots of Alexa488 labeled and unlabeled naive CD4^{+} T-cell cell populations (left panels) and their median indo-1 ratio of Alexa488 labeled CB (solid black line) and unlabeled APB (dashed gray line) naive CD4^{+} T cells (right top panel) versus unlabeled CB and Alexa488 labeled APB CD4^{+} T cells (right bottom panel). (**B**) Mean $[Ca^{2+}]_i$ after CD3 mAb cross-linking is significantly higher in CB naive CD4^{+} T cells compared to those of APB (n=3). (**C**) Alexa488 cell labeling does not have a significant effect on a peak calcium flux of a cell population (n=6). Individual donors are connected by lines. (**D**) Mean $[Ca^{2+}]_i$ following ionomycin addition in CB and APB naive CD4^{+} T cells (n=3). p-values were calculated

using a paired, two-way ANOVA to account for both labeling and sample source. All samples were gated on live, CD8$^-$ CD19$^-$ CD45RO$^-$ MACS-purified naive CD4$^+$ T cells.
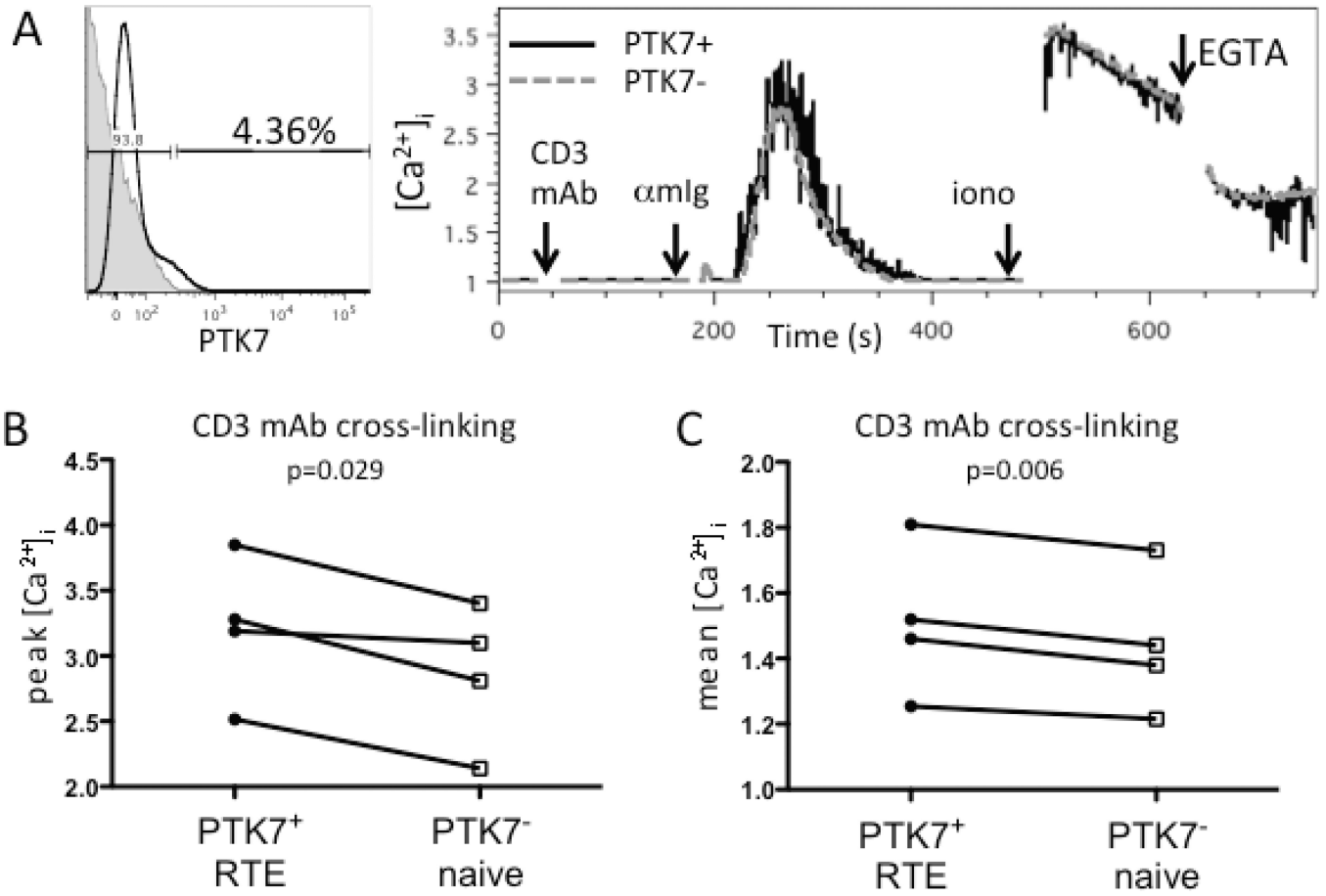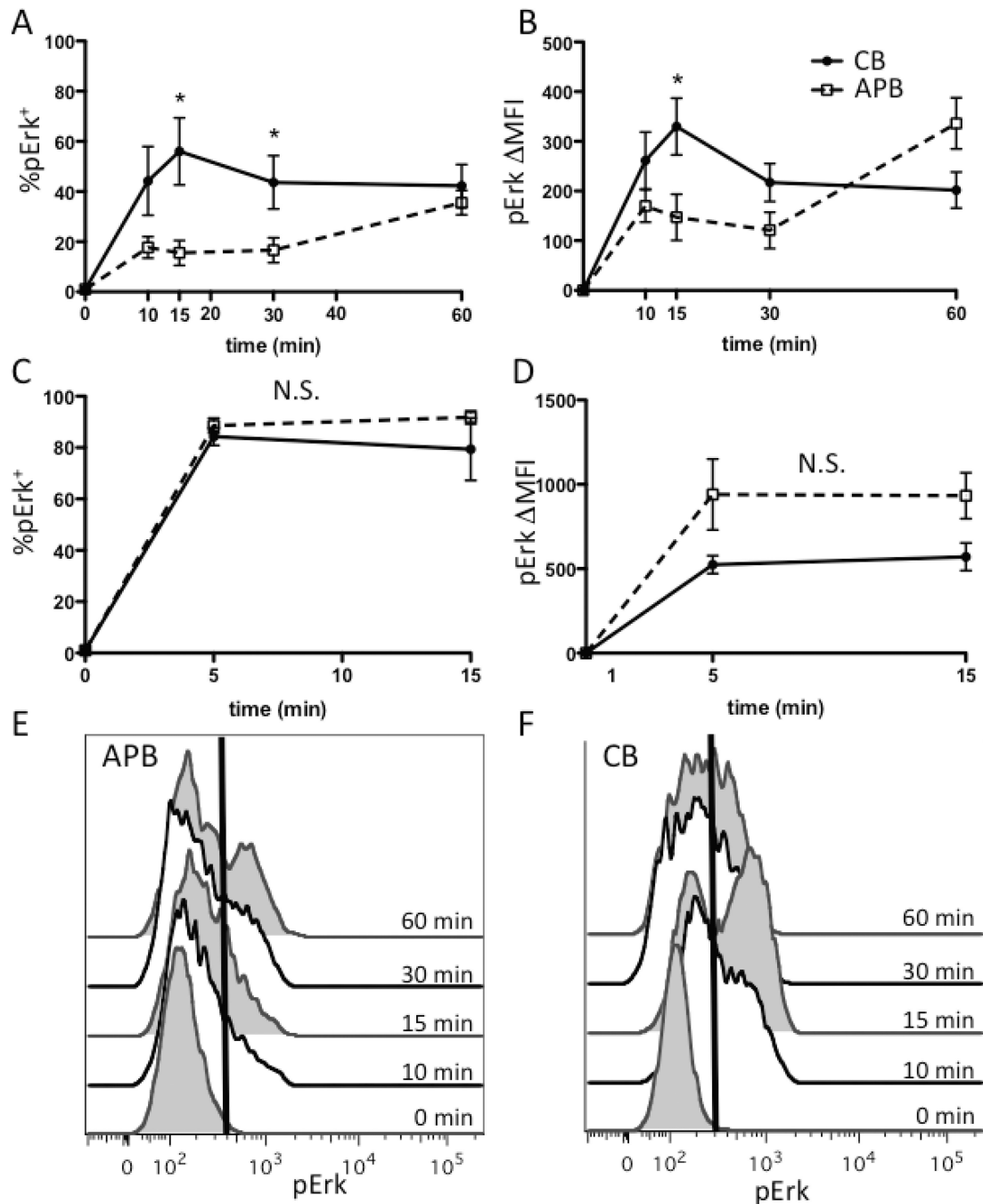
FIGURE 2.
CD4^{+} PTK7^{+} RTEs of APB have higher calcium flux after CD3 mAb cross-linking than more mature naive CD4^{+} T cells. (**A**) Representative flow cytometry plot of PTK7 staining (black line) overlaid on an isotype control stain (filled gray histogram), and kinetics plot of calcium flux after CD3 mAb crosslinking, ionomycin addition, and EGTA addition in samples from an individual adult donor. (**B**) Peak $[Ca^{2+}]_i$ and (**C**) mean $[Ca^{2+}]_i$ of PTK7^{+} naive CD4^{+} T cells (RTE) and PTK7^{−} naive CD4^{+} T cells after CD3 mAb cross-linking (n=4). PTK7^{+} and PTK7^{−} cell populations from the same individual are connected by lines. p-values were calculated using a two-tailed, paired student's t-test. All samples were gated on live, CD8^{−} CD19^{−} CD45RO^{−} purified naive CD4^{+} T cells.

FIGURE 3.
Erk phosphorylation is higher in CB naive CD4^{+} T cells than APB cells. (**A**) %pErk^{+} after stimulation with plate-bound anti-CD3 and anti-CD28 is significantly higher in CB naive CD4^{+} T cells after 15 (p=0.01), and 30 (p=0.03) minutes of stimulation. (**B**) Change in MFI (ΔMFI) is significantly higher (p=0.04) in CB naive CD4^{+} T cells after 15 minutes of stimulation with plate-bound anti-CD3 and anti-CD28. (**C**) %pErk^{+} is not significantly different between CB and APB naive CD4^{+} T cells after stimulation with ionomycin and PMA. (**D**) ΔMFI is not significantly different between CB and APB (p>0.05) after stimulation with ionomycin and PMA. (**E**) Representative plot of pErk staining in one APB

sample stimulated with anti-CD3 and anti-CD28. Time points are alternately filled or white, for clarity. Line indicates position of positive gate. (**F**) Representative plot of pErk staining in one CB sample stimulated with anti-CD3 and anti-CD28. Cells are gated on CD3^{+} CD4^{+} CD45RA^{+} lymphocytes.
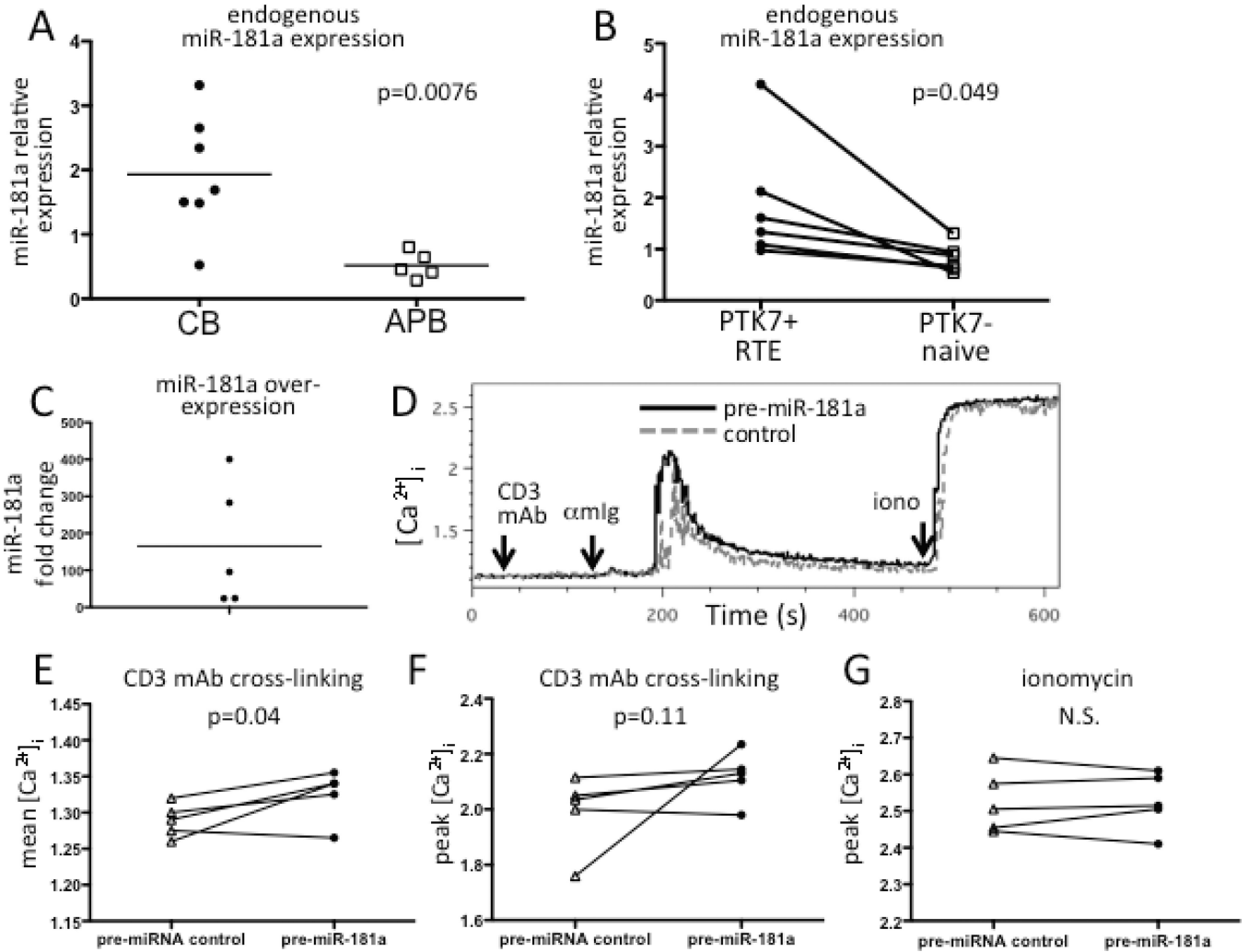
FIGURE 4.
Higher expression of miR-181a in CB naive CD4^{+} T cells regulates calcium flux. (**A**) CB
naive CD4^{+} T cells (n=5) have significantly higher levels of miR-181a expression than those
of APB (n=7). (**B**) miR-181a expression is significantly higher in PTK7^{+} RTEs than in
PTK7- naive CD4^{+} T cells of APB (n=6). Lines indicate samples from individual donors.
(**C**) Transfection with pre-miR-181a RNA results in increased expression of mature
miR-181a. (**D**) Representative $[Ca^{2+}]_i$ plot of replicates of pre-miR-181a transfected (solid
black line) and control pre-miRNA transfected (dashed gray line) APB naive CD4^{+} T cells.
(**E**) Mean and (**F**) peak $[Ca^{2+}]_i$ following CD3 mAb cross-linking from all APB donors was
higher after transfection with the pre-miRNA control or pre-miR181a. (**G**) Peak $[Ca^{2+}]_i$ in
response to addition of ionomycin of CB and APB naive CD4^{+} cells was not different after
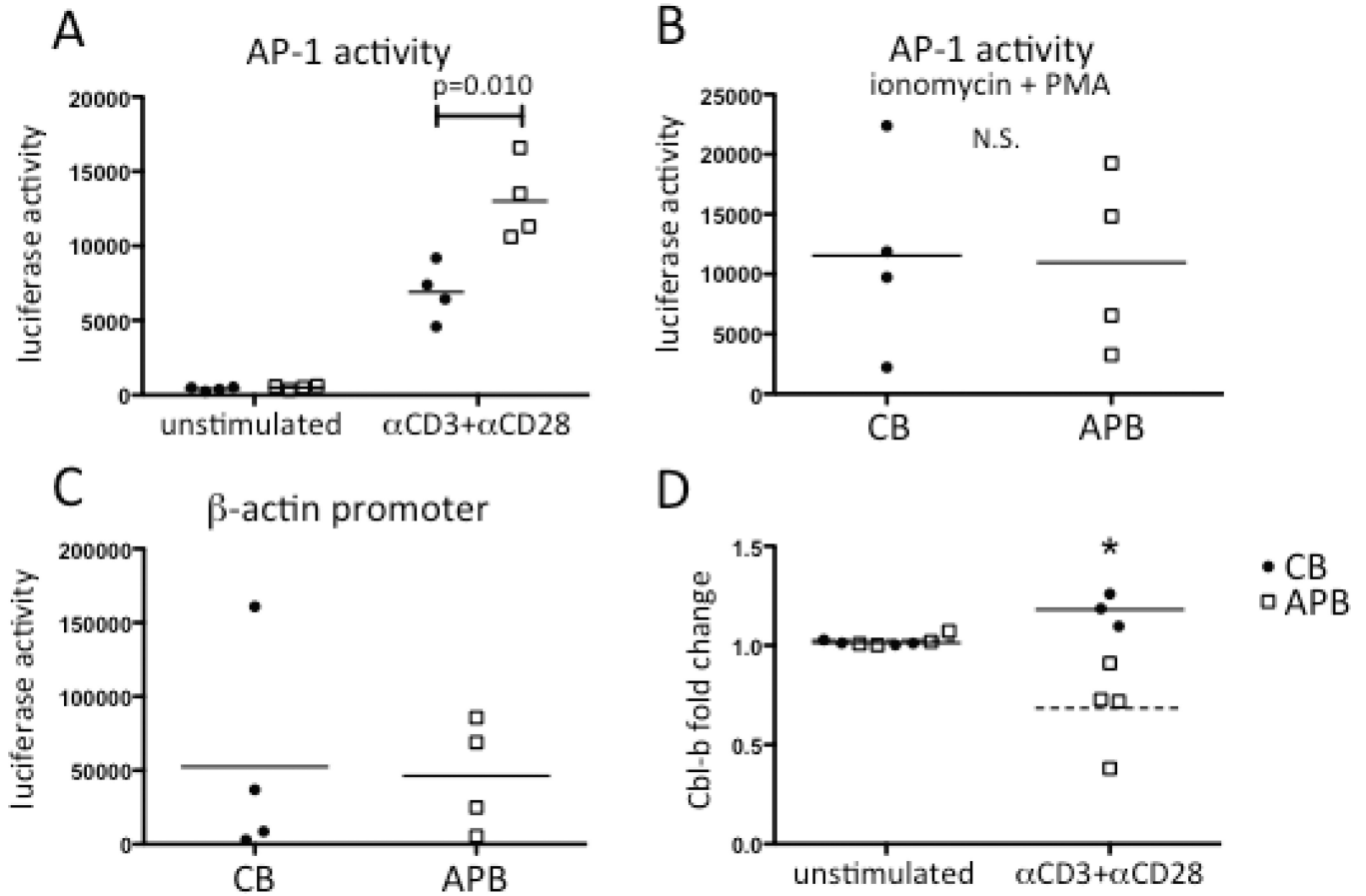transfection with a pre-miRNA control or pre-miR-181a RNA.

Palin et al.   Page 22

FIGURE 5.
AP-1-dependent transcription is reduced in activated CB naive CD4$^+$ T cells compared to those of APB. (**A**) AP-1 reporter luciferase activity in CB (filled circles, n=4) and APB (open squares, n=4) either unstimulated or after 4 hours of stimulation with CD3 and CD28 mAbs. (**B**) AP-1 reporter activity after stimulation with ionomycin and PMA for 4 hours was not significantly different. (**C**) Luciferase activity driven by a β-actin promoter reporter was not significantly different between CB and APB naive CD4$^+$ T cells. (**D**) Cbl-b mRNA was upregulated in CB naive CD4$^+$ T (n=3) cells and downregulated in APB naive CD4$^+$ T cells (n=4) after 4h stimulation with anti-CD3 and anti-CD28 (p=0.025, by a paired Student's t-test).

J Immunol. Author manuscript; available in PMC 2014 March 15.